TOC only

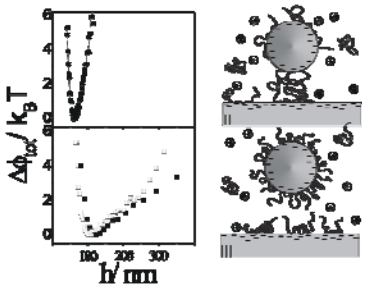

Steric Repulsion by Adsorbed Polymer Layers Studied with Total Internal Interaction Microscopy

Dzina Kleshchanok, Peter R. Lang*

Forschungszentrum Jülich, Institut für Festkörperforschung, Weiche Materie, 52425 Jülich, Germany

Abstract

Total internal reflection microscopy (TIRM) was applied to measure the interaction potential between charge stabilized polystyrene latex spheres and a glass wall in dependence on the concentration of additional polyethylene oxide. The influence of the polymer can be described by steric repulsion between polymer layers, which are physically adsorbed onto the surfaces of the polystyrene sphere and the glass wall. The expected attractive contribution to the potential due to polymer depletion was not observed. An increase of the polymer bulk concentration is shown to strengthen the steric repulsion. At the highest polymer concentrations studied it is possible to accurately describe the experimental data for the steric contribution to the total interaction potential with the Alexander-de Gennes model for brush repulsion.

Keywords: Adsorption; Brush repulsion; Polymer; Colloids; Depletion; Total Internal Reflection Microscopy.

I. Introduction

Interactions in colloid-polymer mixtures are the key question in colloidal stability. Stabilization and destabilization of colloidal systems against van der Waals attraction by

polymers are very important in different fields such as, e. g., food industry, paint production, oil recovery, biology, etc.[1] Two situations, stabilization and flocculation, can be distinguished, depending on whether the polymer adsorbs on the particle surfaces or not. *Adsorption stabilization*, also called steric stabilization, arises in good solvents for the polymer and can be attributed to osmotic interactions between segments of the polymers adsorbed onto opposing surfaces. If the solvent quality for the adsorbed polymer worsens, the repulsive interaction weakens and eventually the particles will aggregate, because steric repulsion can not any more overcompensate van der Waals attraction. This process is usually referred to as *adsorption flocculation.*[2] A second mechanism, which may lead to flocculation even under good solvent conditions is bridging, that is, one polymer chain adsorbs onto two ore more particles simultaneously, thereby causing strong attractive interactions. If the polymer chains do not adsorb onto the colloidal surfaces *depletion flocculation* will take place in the system.[3] In this case attractive interactions are due to a polymer concentration gradient from the bulk to the region between two particles located close to each other. Thus, understanding the influence of additional polymer on colloidal interaction is an important issue and the most basic question is whether or not the polymer adsorbs onto the particle surface.

If the polymer chains do not adsorb onto the surfaces a *depletion force* between the surfaces will occur. The mechanism that is responsible for depletion interaction was first explained by Asakura and Oosawa,[4] and independently by Vrij.[5, 6] It can be understood considering two surfaces immersed in a solution of *non-adsorbing* polymer chains. In the step function approximation the polymer concentration in the depletion layer is zero. Outside this layer the polymer concentration equals the bulk polymer concentration. The thickness of the depletion layer, δ, lies in the range of the radius of gyration of the polymer, R_g. If the depletion layers overlap, the osmotic pressure acting on the surfaces is unbalanced leading to a net attractive osmotic force that pushes the surfaces together.

If the polymer adsorbs onto the particle surface, a plethora of different scenarios may occur which have been treated theoretically.[7] The interaction forces depend on the surface coverage, on whether the polymer chains are physically adsorbed from the solution (a reversible process)[8, 9] or grafted onto the surfaces (an irreversible process)[10-12] and on the quality of the solvent.[8, 9, 13, 14]

If the surfaces are *saturated* by adsorbed polymer chains, which are in *full equilibrium* with the surrounding solution, the forces between two polymer adsorption layers are attractive arising from mainly bridging.[8, 9] Weak repulsion was found at larger separation distances,[15] which, however, is not always strong enough to withstand the van der Waals attraction between the colloidal particles i. e. to stabilize them.[14] Strong attraction due to bridging is usually observed between two undersaturated polymer layers.[16, 17]

In the so-called case of *constrained equilibrium* the rate constant for adsorption is larger than that for desorption, i. e. desorption is kinetically hindered. For this case de Gennes predicted a repulsive interaction for strongly overlapping chains in good solvents. The repulsion arises from the steric interaction between two opposing adsorption layers.[8] In bad solvents a long-ranged attraction is predicted, which turns into a short-ranged repulsion, if the particles are forced close enough to compress the adsorbed polymer layers.[9, 13, 18] Especially the latter situation is relevant, if measurements are performed with surface force apparatus (SFA).[17-20]

If the rate constant for desorption becomes very small, the adsorbed polymer chains may be regarded as being grafted onto the surface. In this case they act as very efficient stabilizers for colloidal particles in the good solvent regime and the particle-particle interaction can be described by the Alexander-de Gennes model for polymeric brushes.[10, 11]

Most direct experimental measurements on the interactions between surfaces bearing adsorbed and grafted polymer chains were done using SFA[17-20] and atomic force microscopy (AFM).[21-24] However, these methods only allow to study large interaction potentials with a high degree of polymer layer compression and interpenetration. Thus, it might be questioned whether experiments performed with AFM and SFA are adequate for weak interactions which are relevant to the behavior and properties of colloidal particles stabilized with polymer layers. Recently measurements with optical tweezers[25] and total internal reflection microscopy (TIRM)[26] were reported. Major advantages of these techniques are their extreme sensitivity and their ability to investigate the interactions of a single, freely moving Brownian particle. For the case of a colloidal particle bearing polymer chains this means there is no external layer compression created under experimental conditions.

In this contribution we report on a systematic TIRM study of the effect of additional polyethylene oxide (PEO) on the interaction between charge stabilized polystyrene (PS) latex spheres and a glass wall. We chose this system, although there had been thorough investigations of it before, because from literature it appears that there are two scientific communities, which have contradicting views of the properties of PEO. Scientists studying polymer adsorption consider PEO as polymer with a high tendency to adsorb from aqueous solutions on such surfaces as: mica,[19, 27] glass,[23] silica[25, 28] and PS[29]. At the same time scientists investigating depletion processes have treated PEO as non-adsorbing on PS and glass surfaces.[30-33] We studied PEO with $M_w = 10^6$ g/mol and for this particular case we will show that depletion interaction in the system *PS sphere/ PEO in water/ glass wall* is very much weaker than expected from the standard theoretical model, if it is active at all. To the contrary we observe repulsive interaction induced by the addition of polymer, which we assign to the formation of a brush-like PEO layer on the particle and the glass surface.

This paper is organized as follows: in section II we present our experimental system and TIRM-equipment. The experimental findings are reported in section III and discussed in their context to work published earlier in section IV. Finally, we give short conclusions in section V.

II. Experimental

II.A. Samples and preparation

Polystyrene sulphonate latex particles with a diameter of 5.7 μm (CV 9.5%) were obtained from Interfacial Dynamics Co., USA and 2.8 μm (σ=0.13 μm) spheres were purchased from Polyscience Inc., USA. The particles were diluted from the stock suspension down to a volume fraction of 10^{-9} for the experiments. The solutions were contained in a carbonized PTFE-frame sandwiched between two microscope slides from BK-7 glass, which were received from Fischer Scientific Co., USA. The glass slides were thoroughly cleaned in an ultrasonic bath for 30 min in ethanol before assembling the sample cell.

Poly(ethyleneoxide) with a molar mass of M_w = 10^6 g/mol (PD < 1.35) was obtained from PSS GmbH, Mainz, Germany and used without further purification. The radius of gyration of this polymer in water was determined by static light scattering as R_g = 67.7 nm for the molar mass of PEO used in our experiments.[34] On the basis of M_w and R_g we estimated $c^* = 3M_p / 4\pi R_g^3 N_A$ as 1.3 g/L. Ultra pure Milli-Q water (resistivity better than 18.2 MΩcm^{-1}; Millipore GmbH, Germany) was used as a solvent for all experiments and cleaning steps. Solutions of PEO were prepared by weight. All polymer concentrations, c_{PEO}, used in the measurements were lower than c^*. The highest bulk polymer concentration of 1.0 g/L is at least three times the concentration necessary to saturate the particle and the wall surfaces, according to literature adsorption isotherms.[35] The pH value and the Debye length of the solutions were adjusted with a standardized stock solution of 0.1 M NaOH from Aldrich,

Germany. All solutions had pH=10.8, corresponding to a Debye length of κ^{-1}=12.4 nm and a NaOH concentration of 0.6 mM, to keep the glass surface negatively charged, which is crucial at the initial and final stages of the experiment. All experiments were performed at ambient temperature.

II.B. TIRM measurements

The interaction potentials between a single particle and the wall were obtained using evanescent field scattering in total internal reflection microscopy (TIRM)[36] For this purpose a laser beam is directed via a prism to the glass/solution interface with an incident angle, θ, such that it is totally reflected. The electric field of the laser beam penetrates the interface causing an evanescent wave, the amplitude of which decays exponentially with the distance from the interface. A single colloidal sphere, interacting with this evanescent wave, will scatter the light depending on its position as[37]

$$I_s(h) = I(h=0)\exp\{-\beta h\}, \tag{1}$$

where h is the distance from the sphere to the wall and β is the inverse penetration depth of the evanescent wave. Recording intensity fluctuations for a sufficiently long period of time provides the probability density of separation distances, which can be converted into a potential energy profile using Boltzmann's equation

$$p(h) = A\exp\left(\frac{-\phi_{tot}(h)}{k_B T}\right), \tag{2}$$

where $\phi_{tot}(h)$ is the total interaction potential, A is a constant normalizing the integrated distribution to unity.

The experimental TIRM setup was the same as described by Kleshchanok *et al.*[38, 39] With this instrument it is possible to exchange solvents while the observed particle is kept in place

by an optical trap. For all experiments we applied an angle of incidence of 62.9 degree, which corresponds to a penetration depth of β^{-1}=224 nm as calculated from the optical path:

$$\beta = \frac{4\pi}{\lambda}\sqrt{(n_1 \sin\theta)^2 - n_2^2}, \qquad (3)$$

where n_1 = 1.330 and n_2 = 1.515 are the refractive indices of the water and the glass respectively. The exact knowledge of the penetration depth is crucial for the data analysis, because it enters into the conversion of intensities to separation distances.[39] We therefore check whether the experimentally determined potential curve from a sphere of known mass in aqueous suspension of known ionic strength fits to the prediction for the potential based on a superposition of gravity and electrostatic repulsion. The influence of the electrolyte and the polymer in the solution on β^{-1} can be neglected. Based on the refractive index increments for NaOH (dn/dc = 2.78×10^{-4} L/g)[40] and PEO (dn/dc=1.35×10^{-5} L/g)[34] we calculate that the variation of n_1 is smaller than 10^{-4} at the highest polymer concentration. A larger effect is expected from the variation of n_1 in the layer of adsorbed PEO on the glass and the particle surface. From the respective adsorption isotherms[29] we estimate $n_1 \approx 1.331$ in the adsorbed polymer layer. Assumption, that the entire gap between the glass and the particle is filled with a medium of this refractive index, would increase the penetration depth by ca. 5%. This does not influence the conversion of scattered intensities to separation distances to a detectable amount. We therefore chose to use n_1 = 1.330 throughout. This 'simplified' approach was also successfully used by Bevan and Prieve who studied the adsorption of Pluronic on the PS surfaces.[26]

The protocol for a complete experimental run was as follows: first a potential was measured in the absence of PEO at a given Debye length. Then the solvent was replaced by a polymer/ electrolyte solution with the same Debye length as before. The potential measurement was performed after a delay time of at least one hour; the time is required for the system at a given concentration to reach equilibrium. The procedure was repeated for seven different polymer

concentrations. Afterwards the polymer was desorbed from the surfaces and at the final stage a solution with a high salt concentration (0.1 M NaCl) was pumped into the sample cell to completely screen the electrostatic interaction. By this the particle is allowed to settle at the wall surface, which enables the measurement of the reference intensity $I(h=0)$, that is required to convert relative separation distances to absolute values. It was possible to use the same particle to obtain a complete set of interaction potentials for different polymer concentrations which largely facilitates comparison between potential profiles recorded under different conditions.

III. Experimental findings

III.A. Temporal evolution of interaction profiles; phenomenological description

In Figure 1.I–1.V we present the time evolution of the interaction potential between a 2.8 μm diameter PS sphere and the wall over a complete experimental run. Part a) shows the experimentally measured interaction potentials and in part b) we display sketches to illustrate the qualitative interpretation of the potentials. Histograms of the intensity fluctuations resulting from the thermal motion of the sphere are shown as insets in Figure 1a.I)–1a.V), where the frequency of certain intensity $N(I)$ is plotted *vs* I. From the histograms we calculated potential profiles, $\Delta\phi_{tot}(h)$, by applying the standard procedure described elsewhere.[36]

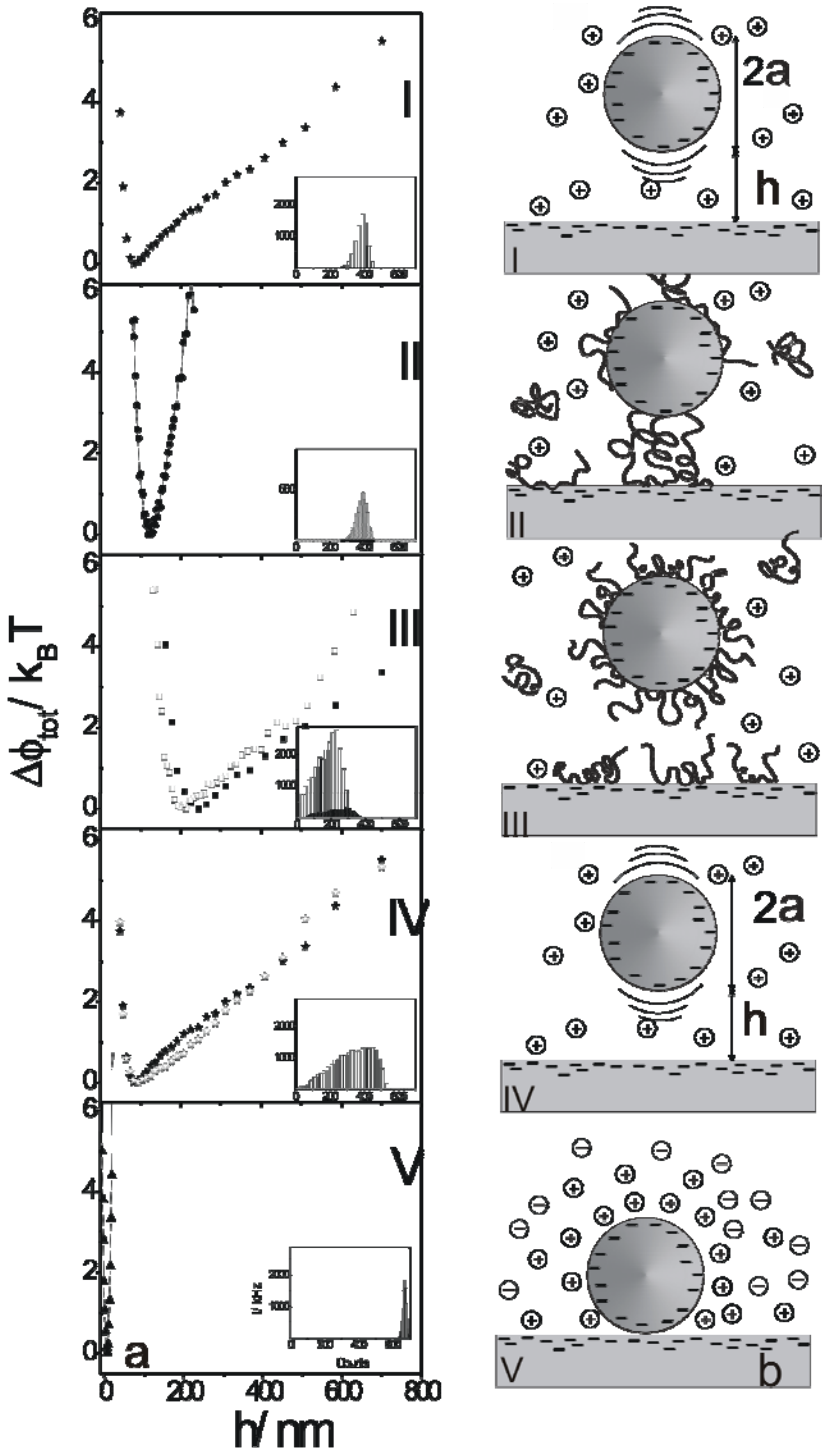

Figure 1. Time evolution of the adsorption process in a system *PS sphere* (2.8 μm)*/ PEO in water/ glass wall*: a) experimental interaction profiles $\Delta\phi_{tot}(h)$; b) sketches illustrating the phenomenological interpretation. For details see main text.

I) In the absence of PEO there are just two contributions to the potential which are gravitational energy $\phi_G(h)$ and electrostatic repulsion $\phi_{el}(h)$:

$$\phi_{tot}(h) = \phi_{el}(h) + \phi_G(h). \quad (4)$$

Since the separation distances were always larger than the range of the van der Waals attraction, the latter is negligible. Figure 1a.I) shows the interaction potential between a sphere and the wall in the absence of PEO.

II) After pumping a PEO solution with a concentration of 1.0 g/L through the cell, the interaction potential becomes narrower an deeper. This could be either due to a depletion effect or to polymer bridging. However, the attractive force is still large at separation distances exceeding 150 nm. At this distance depletion interactions should have leveled off, because the effect of depletion is limited to a range of $2.26 \times R_g \approx 150$nm in the present case. We thus conjecture that bridging interactions are effective in this situation, which result in comparatively small fluctuations of the scattered intensity, a correspondingly narrow intensity histogram and a very narrow and deep potential, which is presented in Figure 1a.II). However, within several minutes, after the surfaces had been saturated with the polymer, the intensity fluctuations become larger again (see also Figure 2) indicating a weakening of the bridging.

III) We now let the system stay for one hour to reach the equilibrium. Afterwards the interaction potential, shown as solid squares in Figure 1a.III), was measured. The minimum position of the potential, i. e. the most probable separation distance of the sphere from the wall is shifted to much higher values as compared to the system which contained no PEO (Figure 1a.I). This indicates an additional repulsive contribution due to steric interaction between adsorbed polymer layers which stabilizes the colloidal particle. To demonstrate the efficiency of the steric stabilization we replaced the solvent by a solution with the same polymer content but now having $c_{NaCl} = 0.1$ mol/L. At this electrolyte concentration the Debye

length[41] $\kappa^{-1} = 0.304/c^{0.5}_{NaCl}$ is of the order of 1 nm which means effective screening of the electrostatic interactions. The empty squares in Figure 1a.III) show the potential measured under these conditions. There is no significant difference between this and the potential obtained in the presence of low electrolyte concentration (0.6 mM NaOH), shown as solid squares. This fact qualitatively indicates that the stability of the colloidal particle is due to steric repulsion between the adsorbed polymer chains and that electrostatic repulsion can be neglected at high polymer concentrations. The slight shift of the minimum position between the two curves is probably caused by a reduction of the range of the steric repulsion, due to a slight desorption of the polymer during solvent replacement. Further it is important to note, that at distances smaller than 200 nm the interaction potential is purely repulsive in both cases. This is not compatible with depletion interaction playing a significant role in this situation. According to the theory for depletion interaction, a potential minimum around $h \approx$ 50 nm with a depth of several $k_B T$ is expected from the polymer concentration at hand. This indicates that depletion interaction plays a minor role, if at all, in the present situation.

IV) Subsequently a solution of 0.6 mM NaOH without PEO was pumped through the cell for four hours to desorb PEO completely from the glass and the PS surfaces. The empty stars in Figure 1a.IV) present the interaction potential between the sphere and the wall after complete desorption. This potential corresponds very well to the potential obtained at stage I) which is presented for comparison as solid stars.

V) After PEO had been desorbed from the surfaces a 0.1 M NaCl solution was added to the cell again. Now the electrostatic repulsion is screened completely, and the particle sticks to the wall, resulting in very small intensity fluctuations. If these fluctuations are analyzed in the usual way, the resulting 'potential curve' becomes extremely narrow (Figure 1a.V). It is important to note that this curve does not represent a real interaction potential but reflects fluctuations of the primary intensity and the thermal noise of the counting statistics.

It is possible to directly observe the transition from bridging between the sphere surface and the wall to additional stabilization by the steric repulsion in the presence of PEO, i. e. from situation II to III in Figure 1. For this purpose we recorded the scattered intensity trace for 30 minutes, shown in Figure 2. The intensity fluctuations are a result of the thermal motion of the particle normal to the wall, which allows a qualitative interpretation of the data by the following considerations. The closer the sphere is to the wall, the higher is the average scattered intensity; and the wider the range of separation distances it is able to probe, the larger are the fluctuation amplitudes.

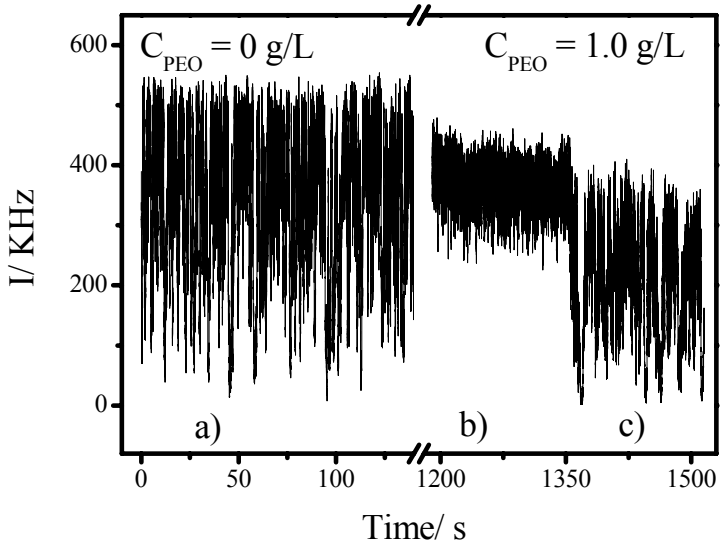

Figure 2. Scattered intensity from a 2.8 μm diameter PS sphere close to the glass wall *vs* time: a) particle in electrolyte solution; b) decrease of the average intensity and fluctuation amplitudes after adding PEO into the system; c) spontaneous increase of the fluctuation amplitude parallel to a decrease of the average intensity.

Part a) of the trace shown in Figure 2 was recorded in the absence of PEO and the intensity profile here corresponds to the potential presented in Figure 1a.I), which consists solely of a superposition of gravity and electrostatic repulsion. After a polymer solution with c_{PEO} = 1.0 g/L was pumped into the cell, bridging occurred. As is shown in Figure 2b), the intensity

fluctuations were damped, which means that the separation distances, the sphere could sample, were very limited. From Figure 1a.II) we can see that they are constricted to ca. 200 nm ≈ $3R_g$. After ca. four minutes the intensity fluctuations spontaneously broadened while the mean value became smaller as shown in Figure 2c). This is in accordance with the transition from a situation with a small amount of polymer adsorbed to the surfaces, where bridging dominates. to a situation with large polymer excess concentration at the surfaces, where steric repulsion dominates. The decrease of the average scattered intensity shows that the most probable separation distance, $h_{\min}$ has increased. This means that the repulsive part of the potential now has a larger range than in the case where electrostatics are the only repulsive contribution (Figure 2a).

Up to now we presented a purely phenomenological discussion of the polymer influence on the interaction between a PS-particle and a glass wall, which may be summarized as follows. The polymer PEO appears to adsorb on the glass an the particle surface, leading to a steric repulsion between the adsorbed polymer layers, while depletion plays a minor role, if it is active at all. To enable a quantitative comparison between experimental data and with theoretical model we measured the dependence on PEO concentration of the interaction potential between the sphere and the wall. However, we chose to use larger colloidal particles in order to enhance possible effects of polymer depletion. As the strength of depletion interactions is expected to scale with the particle radius, we used a particle with a diameter of 5.7 μm. With this particle we observed phenomenologically the same behavior as discussed above for the 2.8 μm sphere. The data for the dependence of the equilibrium potential on the polymer concentration are presented and discussed quantitatively in the next section.

III.B. Interaction profiles at different PEO concentrations

Choice of the model potential. As discussed in the previous section there are two contributions to the total equilibrium interaction potential between the PS-particle and the

glass wall, if no polymer is present, i. e. electrostatic repulsion, and gravity. Upon the addition of PEO to the system, either depletion or steric repulsion or both of them may become active. In Figure 3a) the interaction potential between a 5.7 μm sphere and the glass is plotted for two polymer concentrations, namely c_{PEO} = 0 and c_{PEO} = 1.0 g/L. For comparison we plotted the corresponding data from the 2.8 μm sphere in Fig 3b). In both cases, the data for c_{PEO} = 0 were non-linear least squares fitted with the superposition of a gravitational contribution and an electrostatic term:

$$\phi_{tot}(h) = B\exp(-\kappa h) + G_{eff}h, \tag{5}$$

where $G_{eff} = (4/3)\pi a^3 \Delta\rho g + F_L$ is effective weight of the sphere of radius a, with $\Delta\rho$ the particles excess mass density, g the acceleration of gravity and F_L the light force due to the optical trap. B is the charge parameter, which is difficult to determine independently.[41] It is connected with the most probable separation distance between the particle and the wall $h^0_{\min}$ through

$$\kappa h^0_{\min} = \ln\frac{\kappa B}{G_{eff}}, \tag{6}$$

where the superscript '0' refers to zero polymer concentration. Applying eq 6 we can eliminate B from eq 5 and the relative potential, $\Delta\phi_{tot}(h)$, can be obtained as

$$\frac{\Delta\phi_{tot}(h)}{k_BT} = \frac{G_{eff}}{k_BT}\left(\kappa^{-1}\left[\exp\left\{-\kappa(h-h^0_{\min})\right\}-1\right] + (h-h^0_{\min})\right). \tag{7}$$

where we defined $\Delta\phi(h^0_{\min}) = 0$. Since the Debye length is fixed by the electrolyte concentration to κ^{-1}=12.4 nm we remain with two floating parameters, i.e. h_{eff} and $h^0_{\min}$. The best fits with eq 7 are presented as solid line in Figure 3. The effective weight of the spheres obtained from the fit are G_{eff} = 88 fN for the large and G_{eff} = 37 fN for the small sphere. These

values deviate from the values calculated using the particle radius and the nominal density ρ = 1.05 g/cm^3 because of the contribution of F_L. The minimum positions $h^0_{min} = 129$ nm for the large and $h^0_{min} = 89$ nm for the small sphere can be converted to the charge parameter B=1.3×10^4 k_BT and. B=1.5×10^2 k_BT respectively. We did not correct for the experimental data for the effect of the laser trap because it does not influence the shape of the repulsive branch of the potential, which is the relevant part for the effects to be discussed here. This is illustrated by the curves with small symbols, which have been calculated using the nominal PS density, i. e neglecting F_L.

In order to estimate the influence of depletion interaction upon addition of polymer we calculated the depletion potential according to

$$\frac{\phi_{depl,sphere\text{-}plate}(h)}{k_BT} = \begin{cases} -3\frac{a}{R_g{}^3}\frac{c_p}{c^*}\left[\delta^2 - \delta h + \frac{1}{4}h^2\right] & for\ 0 \le h \le 2\delta \\ 0 & for\ h > 2\delta \end{cases}, \qquad (8)$$

where c^* is the polymer overlap concentration, δ is the depletion layer thickness which depends on the radius of gyration of polymer R_g as $\delta = 2R_g/\sqrt{\pi}$.[42] The strength of the depletion interaction increases with growing polymer concentration; the range of the potential is set by R_g and does not exceed two depletion layer thicknesses.

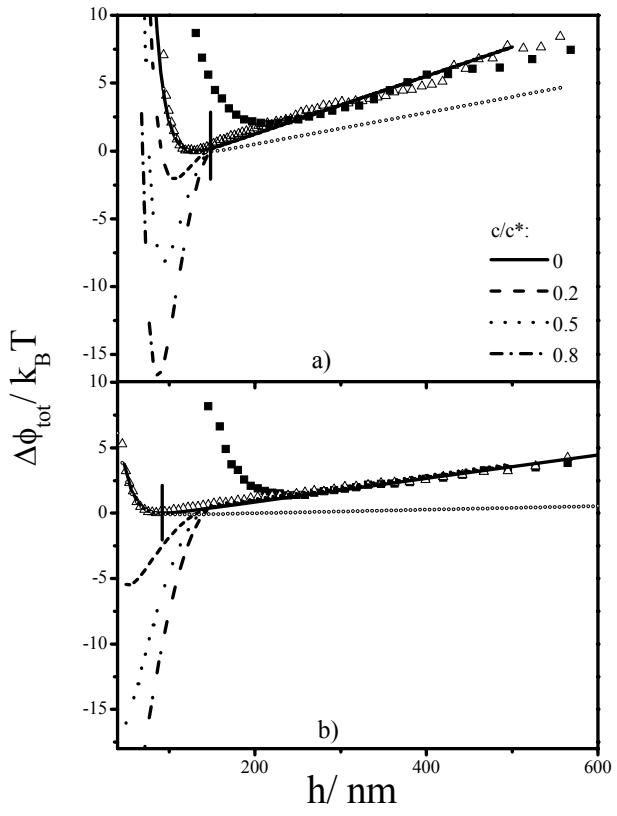

Figure 3. Interaction potentials, $\Delta\phi_{tot}(h)$, between a 5.7 μm (a) and a 2.8 μm (b) diameter PS sphere and a glass wall. Symbols are experimental data recorded at different polymer concentrations; open triangles: c_{PEO} = 0 and full squares: c_{PEO} = 1.0 g/L PEO (c/c* = 0.8). Lines present the calculations according to the superposition of eq 7 and 8 (a: G_{eff} = 88 fN, κ^{-1} = 12.4 nm, $B = 1.3\times10^4\ k_BT$; b: G_{eff} = 37 fN, κ^{-1}=12.4 nm, $B = 1.5\times10^2\ k_BT$ nm) for different polymer concentration as indicated in the figure. The vertical bars mark the separation distance where the electrostatic potential has decayed to 0.1 k_BT.

Superpositions of this contribution with the effective weight and the electrostatic repulsion determined before are displayed as broken lines in Figure 3 for different values of c/c^*. For both spheres the total potential is strongly attractive for distances smaller than ca. 150 nm. Above this value the potential levels off to the effective weight of the spheres. At distances significantly smaller than the respective minima positions, h^0_{min}, the potentials run through a minimum, the depth of which increases with c/c^*. For small separation distances the

theoretical potential become repulsive due to the large electrostatic contribution. It is obvious from Figure 3 that the experimental potential profile for the highest polymer concentration we studied (c/c^* = 0.8), which is displayed as solids squares in Figure 3, has a completely different shape. First, the gradient $d\phi_{tot}(h)/dh$ of the experimental potential is increasing monotonically with the distance, while it has a maximum at in the calculated curves. Second, the position of the potential minimum $h_{\min}$ is shifted to larger values with respect to $h^0_{\min}$ by a factor of two for the larger sphere, while in the case of the small sphere $h_{\min} \approx 3h^0_{\min}$. Differently, for the theoretical curves $h_{\min}$ is always significantly smaller than $h^0_{\min}$. Third, the smallest separation distance, for which we could determine the interaction potential at c/c^* = 0.8, i.e. the smallest distance the particles probe with a significant frequency is about the same distance at which the depletion potential has leveled off to less than 0.1 k_BT, for both the small and the large particle. A similar behavior was observed for all other polymer concentrations.

Further, the shift of the potential minimum position requires the presence of an additional repulsive contribution. This is illustrated by the vertical bars in the two figures, which are located at the position where the electrostatic potential becomes negligible. At these distances the electrostatic potential, as calculated with the parameters determined by the fit to the experimental curve obtained with c_{PEO} = 0, has decayed to 0.1 k_BT. However, the total repulsive contribution is ca. 6 k_BT for the 5.7 μm particle and ca. 20 k_BT for the 2.8 μm particle at the same positions. This shows that we have to account for a steric contribution to the total potential. The relative strength of the steric and the electrostatic repulsion changes with polymer concentration as will be discussed in detail in the following section.

The above considerations lead us to the conclusion that a feasible model for the description of the total interaction potential between the PS particles and the glass wall consists of a superposition of three contributions, i. e. an effective gravitational part, electrostatic repulsion

and steric repulsion. To describe the steric repulsion, we chose the Alexander-de Gennes model for polymer brushes.[10, 11] This is justified by the observation, that it takes several hours of electrolyte solution flow to completely desorb the polymer from the particle and glass surfaces. On the time scale of our experiments it is therefore reasonable to regard the adsorbed polymers as grafted chains.

Thus the model function, which we applied for the non-linear least squares fitting of the potential profiles, was

$$\phi_{tot}(h) = \phi_G(h) + \phi_{el}(h) + \phi_{brush}(h)\,, \tag{9}$$

where the first two terms are given by eq 7 and the contribution of the polymer brushes is given by[43]

$$\frac{\phi_{brush}(h)}{k_B T} = \\ = \frac{32\pi a H_{brush}^2 \sigma^{\frac{3}{2}}}{35}\left[28\left(\left(\frac{2H_{brush}}{h}\right)^{\frac{1}{4}} - 1\right) + \frac{20}{11}\left(1 - \left(\frac{h}{2H_{brush}}\right)^{\frac{11}{4}}\right) + 12\left(\frac{h}{2H_{brush}} - 1\right)\right]. \tag{10}$$

in the range $0 < h \le 2H_{brush}$. Were we used the fact that in the Derjaguin approximation[41] the potential between a planar surface and a sphere is twice as large as between two spheres of equal radius. For $h \le 2a$ the interaction is infinitely repulsive and for $h > 2H_{brush}$ the brush repulsion vanishes. Here σ is the grafting density expressed as a number of brush chains per unit area.

We note that the small deviations from the expected linear behavior of the potential at large distances are not captured by this model. Actually, the physical origin of these deviations is not clear. However, as we have shown for the case of the light force F_L above, small contributions to the total potential at large distances do not influence the shape of the repulsive branch at small distances, which is the only one to be discussed in the following.

Results from model fitting. In Figure 4 we show the experimental interaction potentials between a 5.7 μm sphere and the glass wall for eight different PEO concentrations together with the best fits to the model function of eq 9. Because we had measured the potential profiles for all polymer concentrations with the same particle we fixed the parameter G_{eff} in all fits to the value obtained from fit to the data obtained at $c_{PEO} = 0$. The Debye length was fixed to $\kappa^{-1} = 12.4$ nm, which is the value set by the electrolyte concentration of the solvent, and the particles radius, which enters into the expression for the brush repulsion was fixed to a = 2.85 μm. Thus we were left with four adjustable parameters, i. e. the electrostatic charge parameter, B, the height of the polymer brush, H_{brush}, the brush density σ and the minimum position h_{min}. The latter was restricted to a range of ±5 nm around the minimum position the experimental curves.

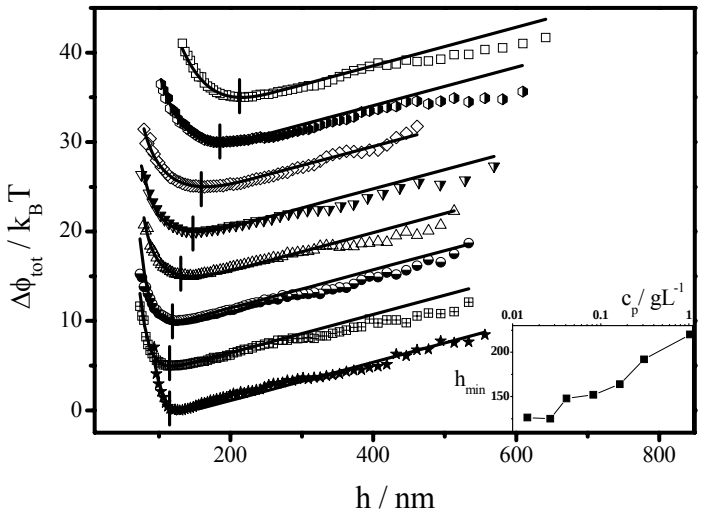

Figure 4. Interaction potentials, $\Delta\phi_{tot}(h)$, between a 5.7 μm diameter PS sphere and a glass wall. Symbols are experimental data obtained at different polymer concentrations are: ★ 0 g/L, ⊞ $1.5\cdot10^{-2}$ g/L, ○ $2.7\cdot10^{-2}$ g/L, △ $4.1\cdot10^{-2}$ g/L, ▼ $8.2\cdot10^{-2}$ g/L, ◇ $1.7\cdot10^{-1}$ g/L; ◐ $3.1\cdot10^{-1}$ g/L; □ 1.0 g/L. The solid curves are the best non linear least squares fits according to eq 9 with the parameters listed in Table 1. For clarity the individual curves have been shifted vertically by 2 k_BT with respect to the curve with the next lower polymer concentration. The

vertical bars mark the most probable separation distance h_{min} obtained from the fit. Inset: h_{min} *vs* bulk polymer concentration c_{PEO}.

The resulting values of the fit parameters are listed in Table 1. The confidence intervals of the individual parameters were obtained by varying one parameter while all others were fixed, until the mean square of the fit increased by thirty percent.

Table 1. Parameters from the non-linear least squares fitting of eq 9 to the experimental interaction potentials, $\Delta\phi_{tot}(h)$, between a PS sphere and a glass wall; top part: 5.7 μm particle diameter; bottom part: 2.8 μm particle diameter. The parameters with an asterisk were kept fix. Values in parenthesis could be varied by more than 100 %, keeping the other parameters fix, without changing the quality of the fit.

c_{PEO} g/L	G_{eff} fN*	κ^{-1} nm*	B k_BT	h_{min} nm	H_{brush} Nm	σ nm^{-2}
0	88	12.4	12717±3000	129±5	0	0
$1.5\cdot10^{-2}$	88	12.4	3473±800	126±7	(11±11)	$(1.5\cdot10^{-5}\pm1.5\cdot10^{-5})$
$2.7\cdot10^{-2}$	88	12.4	3891±600	125±10	(23±23)	$(9.8\cdot10^{-6}\pm9.8\cdot10^{-6})$
$4.1\cdot10^{-2}$	88	12.4	2479±1000	148±15	117±5	$6.1\cdot10^{-6}\pm5.0\cdot10^{-7}$
$8.2\cdot10^{-2}$	88	12.4	1734±600	152±15	118±4	$6.9\cdot10^{-6}\pm6.0\cdot10^{-7}$
$1.7\cdot10^{-1}$	88	12.4	960±900	164±20	122±3	$7.7\cdot10^{-6}\pm4.0\cdot10^{-7}$
$3.1\cdot10^{-1}$	88	(12.4)	(5184±5184)	192±25	127±3	$1.1\cdot10^{-5}\pm1.0\cdot10^{-6}$
1.0	88	(12.4)	(9617±9617)	220±15	137±2	$1.4\cdot10^{-5}\pm5.0\cdot10^{-7}$
0	37	12.4	150±20	89	0	0
1.0	37	(12.4)	(150±150)	243±20	148±5	$1.8\ 10^{-5}\pm1.0\cdot10^{-6}$

As a general trend we observed that the charge parameter, B, i. e. the strength of the electrostatic repulsion decreases with increasing c_{PEO}. For the two highest polymer concentrations we have set B into parenthesis, because it does virtually not influence the quality of the fit. It could as well be increased by more than 100% as be set to zero (keeping the other parameters fixed) without changing the quality of the fit. That is, at these polymer concentrations the electrostatic repulsion is negligible and the parameter k^{-1} does not have any significance in this case. This is in agreement with our observation that the PS particle was stable even at an electrolyte concentration of 0.1 mol/L, as was discussed in section III. A.

The opposite trend was observed for the brush repulsion. At the two lowest finite polymer concentrations the value of the brush density σ, can be chosen almost arbitrarily without changing the fit result. Accordingly the brush repulsion does not play a role at very low c_{PEO} and the value of the brush height does not have any meaning. This is also reflected in the fact that the minimum position $h_{\min}$ is not significantly changed by the polymer concentration in this range. However at $c_{PEO} > 0.04$ g/L. the reliability of σ increases drastically, and the brush density increases monotonically with polymer concentration. The brush height follows the same trend. These findings indicate that, both the strength of the brush repulsion, which is determined by σ, and the range which depends on H_{brush}, increase with the polymer concentration. This also explains the trend which the minimum position follows with c_{PEO}. As brush repulsion becomes effective, $h_{\min}$ increases monotonically with polymer concentration.

The highest c_{PEO} we applied in the experiments with the large sphere is equal to the polymer concentration, which was used in the experiment on the temporal evolution of the potential profile with the small spheres (see section III. A.). It is thus helpful to compare the results for the two sphere sizes. In the bottom part of Table 1 we listed the parameters for the interaction potential of the small sphere with the glass wall for zero polymer concentration and for $c_p/c^* = 0.8$. Also in this case we observe that the electrostatic repulsion at high polymer concentration

is negligible. The parameters values for the brush height and the brush density are some what higher than, but still in reasonable agreement with those observed with the large sphere at the same polymer concentration. The high value of the minimum position in the potential from the small sphere is due to the reduced strength of the attractive contribution. Thus in both cases we observed a transition from a situation at low polymer concentration where the colloidal particle is stabilized mainly by electrostatic repulsion to a situation where the stabilization is due to steric repulsion alone.

IV Discussion

The experimental findings described above show that the influence of additional PEO on the interaction potential between a PS particle and a glass wall mainly consists in the introduction of an additional repulsive contribution, which can be described with the model for brush repulsion, while polymer depletion appears to be negligible. This is in accordance with former publications, where depletion was not detected;[19, 25, 27] For instance, Klein *et al*[19] and later Luckham *et al*[27] studied adsorption and depletion processes in a solution of PEO using SFA; Braithwaite *et al*[23] applied AFM to study steric interactions between adsorbed PEO layers. In none of these cases any attractive force was observed in the system. One might conjecture that the expected value of the depletion is smaller than the inherent detection limit of these techniques, although depletion was observed with AFM in different systems.[44] Moreover, Owen *et al*[25] used optical tweezers, which enable the detection of forces in the pN-range, to measure interactions between two silica spheres immersed in a solution of PEO and found only a long-ranged steric repulsion.

Anyhow, the negligible contribution of depletion interaction in our measurements appears to be unexpected at first glance, since even at full surface coverage the number of polymer chains which are adsorbed to the surfaces is negligible compared to their total number. Further, the potentials measured in the absence of polymer show a minimum position of $h^0_{\min}$

≈ 130 nm for the 5.7 μm sphere, which is smaller than 2δ for the PEO used here. In an earlier contribution[39] we have shown that depletion interaction should be detectable under these circumstances, if it is larger than approximately k_BT. Calculations show with eq 8 show that the latter criterion for the present polymer/ colloid system is met only for polymer concentrations $c_{PEO} \geq 0.06$ g/L ($c/c^* = 0.05$). In this concentration range however the experimental value of h_{min} is significantly larger than 2δ and depletion interaction is not expected to be observable. On the other hand it might well be that the model of ideal monodisperse chains and hard impenetrable spheres, on which eq 8 is based, is not appropriate to describe depletion for the case of colloidal spheres with polymer chains attached to the surface. It is common understanding that depletion in this situation is much weaker than in the impenetrable sphere case due to the diffuse density profile at the outer side of the polymer layer, which is also verified by the simulations.[45] This would be an alternative explanation for the negligible depletion contribution in our system. However, as to our knowledge there is no theory for the depletion interaction between polymer covered particles.

Nevertheless, the absence of depletion interaction, we observed in the present system, is in contradiction to earlier work by Rudhardt and Bechinger *et al*. These authors report two experiments in which they find strong depletion interaction between PS spheres of different size and a glass wall in the presence of PEO. However, in the light of more recent developments of the theory of polymer depletion, at least the results of their first experiment[30] in which they measure the potential of a 3 μm diameter sphere in presence of PEO chains with a radius of gyration of R_g = 101 nm may be questioned. The experimental potential profiles were analyzed using the Askura-Osawa-Vrij model, in which the polymers are approximated by freely overlapping spheres (FOS). Non-linear least squares fitting yielded r = 150 nm for the FOS radius. At that time Rudhartdt *et al* conjectured that the radius of FOS does not necessarily have to be equal to R_g. However, model calculations with the more recent

exact theory for depletion interaction,[42] i.e. eq 8 shows that depletion is negligible under the reported conditions if the real value for R_g is used. It is therefore rather likely that Rudhardt *et al* observed polymer bridging rather than depletion. In their second paper[31] they investigated the potential of a 10 μm diameter sphere in presence of PEO chains with R_g = 68 nm. To overcome the huge gravitational contribution of this large sphere they reduced the density difference between the solvent and the sphere by mixing water with D_2O, to obtain an effective weight of G_{eff} = 10.3 fN. At the same time the sphere was extremely weakly charged, i. e. $B = 4.8\ k_BT$. This results in a comparatively weak electrostatic repulsion and a small value of $h^0_{min} \approx 40$ nm. As the contact potential of depletion interaction scales with the radius of the particle it might well be strong enough to show up under these conditions, even if it is weaken by the presence of polymer chains adsorbed to the surfaces. On the other hand it can not be ruled out completely that the observed attraction is due to bridging also in this case, as we observe in the early stage of our experiments described in section III.A. Probably the effect of polymer bridging deserves much more systematic investigations, especially as there are analytical theories available nowadays to describe that effect.[46]

Conclusions

We measured the effect PEO on the interaction potential between a charge stabilized PS sphere and a glass wall with total internal reflection microscopy. The time evolution of the potential profile after the addition of the polymer to the solution was followed directly using the scattered intensity fluctuations profile. An attractive bridging interaction was observed in the initial stage, which spontaneously transforms to a steric repulsion within several minutes at constant polymer concentration. An increase of the polymer concentration in the system causes the repulsive interaction between the sphere and the wall to strengthen and the most probable separation distance to become larger. At high polymer concentrations steric repulsion is strong enough to render electrostatic repulsion negligible. In this region it is

possible to accurately describe the experimental data for the steric contribution to the total potential with the Alexander-de Gennes model for brush repulsion.

Acknowledgement

We thank Remco Tuinier for many fruitful discussions.

References

1. Napper, D. H. *Polymeric Stabilization of Colloidal Dispersions*. Academic Press: London, 1983.

2. Hiemenz, P. C.; Rajagopalan, R. *Principles of Colloid and Surface Chemistry*. 3rd ed.; Marcel Dekker Inc.: New York, 1997; p 672.

3. Tuinier, R.; Rieger, J.; de Kruif, C. G. *Adv. Colloid Interface Sci* **2003,** 103, 1-31.

4. Asakura, S.; Oosawa, F. *J. Chem. Phys.* **1954,** 22, 1255-1256.

5. Vrij, A. *Pure Appl. Chem.* **1976,** 48, 471-483.

6. de Hek, H.; Vrij, A. *J. Colloid Interface Sci.* **1981,** 84, 409-422.

7. Netz, R. R.; Andelman, D. *Phys. Rep.* **2003,** 380, 1-95.

8. de Gennes, P. G. *Maromolecules* **1982,** 15, 492-500.

9. Scheutjens, J. M. H. M.; Fleer, G. J. *Macromolecules* **1985,** 18, 1882-1900.

10. Alexander, S. *J. Phys.* **1977,** 38, 983-987.

11. de Gennes, P. G. *Acad. Sci. Ser. II, Fascicule B Mechanique Physique Chimie Astronomie* **1985,** 300, 839-843.

12. Zhulina, E. B.; Borisov, O. V.; Priamitsyn, V. A. *J. Colloid Interface Sci.* **1990,** 137, 495-511.

13. Klein, J.; Pincus, P. A. *Macromolecules* **1982,** 15, 1129-1135.

14. Klein, J.; Rossi, J. *Macromolecules* **1998,** 31, 1979-1988.

15. Semenov, A. N. *J. Phys. II* **1996,** 6, 1759-1780.

16. Rossi, G.; Pincus, P. A. *Macromolecules* **1989,** 22, 276-283.

17. Klein, J.; Luckham, P. F. *Nature* **1984,** 308, 836-837.

18. Klein, J. *Nature* **1980,** 288, 248-250.

19. Klein, J.; Luckham, P. F. *Nature* **1982,** 300, 429-431.

20. Israelachvili, J. N.; Tandor, R. K.; White, L. R. *Nature* **1979,** 277, 120-121.

21. Biggs, S. *Langmuir* **1995,** 11, 156-162.

22. Kelley, T. W.; Schorr, P. A.; Johnson, K. D.; Tirrel, M.; Frisbie, C. D. *Macromolecules* **1998,** 31, 4297-4300.

23. Braithwaite, G. J. C.; Howe, A.; Luckham, P. F. *Langmuir* **1996,** 12, 4224-4237.

24. Yamamoto, S.; Ejaz, M.; Tsujii, Y.; Matsumoto, M.; Fukuda, T. *Macromolecules* **2000,** 33, 5602-5607.

25. Owen, R. J.; Crocker, J. C.; Verma, R.; Yodh, A. G. *Phys. Rev. E* **2001,** 64, 011401.

26. Bevan, M. A.; Prive, D. C. *Langmuir* **2000,** 16, 9274-9281.

27. Luckham, P. F.; Klein, J. *J. Colloid Interface Sci* **1987,** 117, 149-158.

28. Killmann, E.; Maier, H.; Kanuit, P.; Gutling, N. *Colloids Surf.* **1985,** 15, 261-276.

29. Pelssers, E. G. M.; Cohen-Stuart, M. A.; Fleer, G. J. *Colloids Surf.* **1989,** 38, 15-25.

30. Rudhardt, D.; Bechinger, C.; Leiderer, P. *Phys. Rev. Lett.* **1998**, (81), 1330-1333.

31. Rudhardt, D.; Bechinger, C.; Leiderer, P. *J. Phys.: Condens. Matter* **1999,** 11, 10073-10078.

32. Bechinger, C.; Rudhardt, D.; Leiderer, P.; Roth, R.; Dietrich, S. *Phys. Rev. Lett.* **1999,** 83, 3960-3963.

33. Ohshima, Y. N.; Sakagami, H.; Okumoto, K.; Tokoyda, A.; Igarashi, T.; Shintaku, K. B.; Toride, S.; Sekino, H.; Kabuto, K.; Nishio, I. *Phys. Rev. Lett.* **1997,** 78, 3963-3966.

34. Devanand, K.; Selser, J. C. *Macromolecules* **1991,** 24, 5943-5947.

35. van der Beek, G.; Cohen-Stuart, M. A. *Journal de Physique* **1988,** 49, 1449-1454.

36. Prieve, D. C. *Adv. Colloid Interface Sci.* **1999,** 82, 93-125.

37. Prieve, D. C.; Walz, J. Y. *Appl. Opt.* **1993,** 32, 1629-1641.

38. Kleshchanok, D.; Wong, J. E.; von Klitzing, R.; Lang, P. R. *Progr Colloid Polym. Sci.* **2006,** 133, 52-57.

39. Kleshchanok, D.; Tuinier, R.; Lang, P. R. *Langmuir* **2006,** 22, 9121-9128.

40. Weast, R. C. *Handbook of Chemistry and Physics*. 56th ed.; CRC Press, Inc.: Cleveland, 1975.

41. Israelachvili, J. N. *Intermolecular and Surface Forces*. 2nd ed.; Academic Press: London, 1991.

42. Tuinier, R.; Vliegenthart, G. A.; Lekkerkerker, H. N. W. *J. Chem Phys.* **2000,** 113, 10768-10775.

43. Likos, C. N.; Vaynberg, K. A.; Löwen, H.; Wagner, N. J. *Langmuir* **2000,** 16, 4100-4108.

44. Milling, A.; Biggs, S. *J. Colloid Interface Sci* **1995,** 170, 604-606.

45. Striolo, A. *Phys. Rev. E* **2006,** 74, 041401.

46. Bhatia, S. R.; Russel, W. B. *Macromolecules* **2000,** 33, 5713-5720.